AIChE

Control and Enhancement of Permselectivity of Membrane-Based Microcapsules for Favorable Biomolecular Transport and Immunoisolation

Sudhir H. Ranganath, Ai Ling Tan, Fang He, and Chi-Hwa Wang
Dept. of Chemical and Biomolecular Engineering, National University of Singapore, Singapore 117576, Singapore

William B. Krantz
Dept. of Chemical and Biological Engineering, Engineering Center, University of Colorado, Boulder, CO 80309-0424

DOI 10.1002/aic.12525
Published online February 15, 2011 in Wiley Online Library (wileyonlinelibrary.com).

The success of membrane-based, cell-encapsulating microcapsules depends on the membrane permselectivity that provides efficient inward transport of nutrients, therapeutic protein egress, and complete exclusion of immunoglobulins. Microcapsules with a calcium crosslinked alginate core and a genipin-crosslinked chitosan alginate (GCA) were prepared with good control over size, membrane thickness and density. Importantly, in this study, we report a novel approach of using three relevant biomolecules and investigating the effects of the membrane characteristics (thickness and density) and microcapsule size on biomolecular mass transport across the GCA microcapsules using mathematical models based on a balance of the chemical potential. Scaling analysis was used to interrelate the membrane thickness, chitosan–alginate reaction rate constant, and diffusion coefficient. The resistance to diffusion of the three biomolecules increased with membrane density and thickness. Interestingly, swelling in the large microcapsules resulted in an increase in permeability, allowing larger biomolecules (immunoglobulin and carbonic anhydrase) to diffuse more readily. In the case of the smaller biomolecule, vitamin B_{12}, a shorter diffusion path length in smaller microcapsules allowed better ingress. When compared with other microcapsules, the GCA microcapsules possess improved permselectivity for them to allow diffusion of small nutrient molecules and proteins, whereas completely excluding antibodies. Also, these results elucidate the importance of membrane properties and microcapsule size to realize favorable transport of biomolecules. © 2011 American Institute of Chemical Engineers *AIChE J,* 57: 3052–3062, 2011

Keywords: microcapsules, protein delivery, mass transfer, permeability, genipin-chitosan membrane

Introduction

Cell microencapsulation is a membrane-based technology that provides localized and controlled delivery of physiologically bioactive or "de novo" therapeutic proteins from encapsulated genetically engineered cells and immunoisolation. It has demonstrated exciting prospects in diverse biomedical applications[1–6] since the pioneering work of microencapsulating islets[1] over the past three decades. However, extensive clinical success has not been achieved because of inefficient immunoisolation, poor mechanical stability, bioincompatibility, and mass transport limitations.

Correspondence concerning this article should be addressed to C.-H. Wang at chewch@nus.edu.sg.

Alginate microcapsules with a poly-L-lysine (PLL) membrane coating or Alginate Poly-L-lysine Alginate (APA) microcapsules were developed[1] and widely used for cell microencapsulation.[7–11] Unfortunately, PLL has been reported to trigger a fibrotic immune-reaction[12,13] and death of encapsulated cells.[9] Also, insufficient mechanical stability[14,15] and degradation[12] of the PLL membrane cause destabilization of the microcapsules resulting in limited graft survival and adverse immune responses. These serious drawbacks have motivated the exploration of chitosan as an alternative to PLL. Because of its natural origin, abundance, low toxicity, and biocompatibility, chitosan has been used as the polycation to form an alginate–chitosan (AC) complex and investigated for drug delivery[16] and cell encapsulation applications.[17,18] To further reinforce capsular strength, slow down the chitosan biodegradation rate and bring about selective membrane permeability, crosslinking of chitosan with genipin was introduced.[19] The covalent crosslinking of chitosan with genipin, a naturally derived aglucone of geniposide[20] has the proven advantage of extremely low cytotoxicity.[19] The most striking feature of a genipin crosslinked chitosan membrane is its fluoregenic property that enables effective characterization of the membrane[21] and consequently the permeability. Recently, genipin crosslinked alginate–chitosan (GCA) microcapsules have been reported to possess improved membrane strength and reduced capsular swelling and thus have great potential for live cell therapy applications.[22] However, studies of the membrane permeability and diffusion characteristics of GCA microcapsules are lacking. Thus, the mass-transfer properties of GCA microcapsules need to be investigated to systematically develop GCA microcapsules for clinical uses.

Several indices have been used to characterize the mass transport through semipermeable membranes in microcapsules. A new mathematical model was developed by Takashi et al.[23] to predict mass transport of molecules across microcapsules based on the assumption of a local equilibrium state, in which there exists uniformity in solute concentration in the core and the bulk, but a concentration gradient within the membrane that actuates the diffusion across the microcapsule. Ultimately, the diffusion gradually drives the system toward a global equilibrium state. Importantly, Kaminski et al.[24] have shown that the cationic charge density of crosslinked chitosan membranes is very low at pH 7.4; hence, the electrostatic interaction between the genipin-chitosan membrane and the negatively charged biomolecules can be safely assumed to be very low. Accordingly, solute release from a microcapsule and solute diffusing into a microcapsule[25] can be expressed by Eqs. 1 and 2, respectively:

$$C_S(t) = C_S^{eq}(1 - e^{-t/\tau}) \tag{1}$$

$$C_S(t) = C_S^{eq}\left(1 + \left(\frac{C_S^0}{C_S^{eq}} - 1\right)e^{-t/\tau}\right) \tag{2}$$

where $C_S(t)$ is the solute concentration in the extra-capsular medium (mg/ml) at time t, C_S^{eq} is the equilibrium solute concentration in the extra-capsular medium (mg/ml), C_S^0 is the initial solute concentration in the extra-capsular medium (mg/ml), and τ represents the characteristic time that is expressed as:

$$\tau = \frac{rl}{3D_m}\frac{\mu_m'}{\mu_c'} \tag{3}$$

where r is the inner radius of the microcapsule, l is the membrane thickness, D_m is the diffusion coefficient of the solute in the membrane, μ_m' and μ_c' are the concentration derivatives of the solute chemical potentials in the membrane and inner medium expressed as $d(\mu_m C_m^{eq})/dC_m$ and $d(\mu_c C_c^{eq})/dC_c$, respectively, where μ_m and μ_c are the solute chemical potentials in the membrane and inner medium, respectively. For a given solute, the ratio μ_m'/μ_c' is a constant; hence, τ is primarily related to the diffusion coefficient of the solute in the membrane for nonswellable microcapsules. However, it should be noted that for swellable microcapsules, τ can depend on r, l, and D_m.

We intend to explore the application of GCA microcapsules as implantable micro-bioreactors delivering anti-angiogenic proteins for treating malignant brain tumors. However, an evaluation of the membrane permselectivity to various biomolecules is critically essential. Hence, in this study, the mass-transport properties of GCA microcapsules with varying size, membrane thickness, and density were investigated. Scaling analysis was used to develop an equation interrelating the membrane thickness, chitosan-alginate reaction rate constant, and diffusion coefficient. Three biomolecules covering a range of molecular weight, size, charge, and conformation were used to evaluate their ability to diffuse across these GCA microcapsules. The kinetic ingress/egress data of the biomolecules were fitted with the mathematical models based on chemical potential balance to estimate the characteristic time. Finally, the effects of microcapsule size, membrane density, and thickness on the biomolecular mass transport were investigated.

Materials and Methods

Materials

Low-viscosity sodium alginate (~250 cP, 2% at 25°C) was purchased from Sigma-Aldrich. Chitosan with an 80% degree of deacetylation and genipin ($C_{11}H_{14}O_5$, M_W of 226.23) were purchased from Wako Bioproducts, Japan. Acetic acid (99.8%) was purchased from Honeywell, Seezle, Germany and phosphate-buffered saline (PBS) was purchased from First Base. Calcium chloride was bought from Merck, Darmstadt, Germany. Vitamin B_{12} powder, carbonic anhydrase (CA) (from bovine erythrocytes), and human immunoglobulin-G (IgG) were purchased from Sigma-Aldrich. All other reagents were of analytical grade.

Fabrication of genipin crosslinked chitosan–alginate (GCA) microcapsules

GCA microcapsules were fabricated in three steps. The first step involves formation of monodisperse sodium alginate droplets using an electrospray process followed by Ca^{2+} ionotropic gelation of the droplets as depicted in Figure 1A. Briefly, the electrospray setup consists of a pump equipped with a syringe filled with 1.5% (w/v) sodium alginate solution and a needle (22G) connected to high voltage generators (Glassman High Voltage, NJ). By applying a high potential difference to the needle that causes a controlled flow

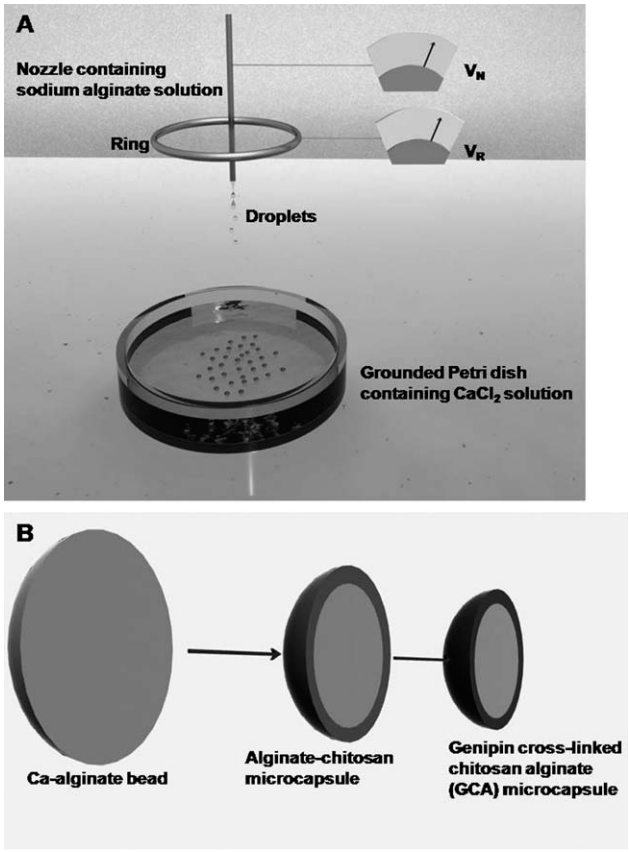

Figure 1. Fabrication of genipin-chitosan-alginate microcapsules.

A: 3-D illustration of the electrospray process for producing calcium crosslinked alginate beads. B: 3-D illustration of the cross-sectional view of the microcapsules after each reaction step.

instability, the jet of alginate solution breaks up into microdroplets. These can be drawn towards a Petri dish containing a $CaCl_2$ solution that rests on a grounded platform. The droplets undergo instantaneous gelation with the Ca^{2+} ions thereby creating calcium crosslinked alginate hydrogel beads. The resulting microcapsules must be thoroughly washed with deionized water to remove any excess Ca^{2+} ions. The microcapsule size can be controlled by varying the nozzle voltage (V_N), ring voltage (V_R), and solution flow rate. Table 1 summarizes the electrospray process parameter values used to fabricate microcapsules in size ranges of 200–300 μm and 500–600 μm, referred to as small and large, respectively. The second step involves treating the calcium crosslinked alginate beads with 10 mg/ml of chitosan solution (with 11 mg/ml of $CaCl_2$ in 1% acetic acid, and pH 5.6–6.0). The coacervation reaction with chitosan was carried out for either 15 min or 30 min at 37°C and 120 rpm that resulted in an AC co-acervated complex shell as depicted in Figure 1B. Thereafter, the microcapsules were washed twice using deionized water to remove traces of any unreacted chitosan. The third step involves reacting the AC microcapsules with 5 mg/ml of genipin solution for 6, 12, or 18 h at 37°C and 120 rpm in an incubator shaker (New Brunswick Scientific, USA) to form GCA microcapsules with a genipin crosslinked chitosan membrane shell as shown in Figure 1B. The microcapsules then were washed with deionized water to remove any unreacted genipin and then stored in deionzed water for subsequent use. Various types of GCA microcapsules were produced with two sizes (small and large), two different membrane thicknesses (determined by chitosan-alginate reaction time) and three levels of genipin-chitosan membrane crosslinking density (determined by the genipin crosslinking reaction time with chitosan) as summarized in Table 2, then washed with deionized water to remove any unreacted genipin and stored in DI water for further use.

Table 1. Operating Parameters of the Electrospray Process

Size of Microcapsules (μm)	Solution Flow Rate (ml/h)	Nozzle Voltage Relative to Ground, V_N (kV)	Ring Voltage Relative to Ground, V_R (kV)
200–300	0.5	11.5	0
500–600	0.6	11.6	9.6

Microcapsule and membrane characterization

The thickness and crosslinking density of the fluoregenic genipin-chitosan membrane were characterized using a Nikon A1 confocal microscope (Nikon, Japan) equipped with a Nikon Eclipse TE2000-E inverted microscope and a multiline argon laser. For image acquisition, the microcapsules were placed on a Menzel-Glaser cover slip in the presence of deionized water. A single green fluorescence mode at an excitation of 488 nm with an emission filter at 500–550 nm was used to scan the samples in galvano mode. An equatorial section of the microcapsules was chosen as the focal plane and all the images were acquired by keeping the microscope settings and laser power constant to ensure comparable images. NIS elements software was used to acquire and analyze the fluorescence intensity profiles corresponding to the line across the focal plane of the microcapsules. The size of the microcapsules was also quantified using NIS elements ($N = 50$).

Biomolecular ingress into GCA microcapsules

Three biomolecules, vitamin B_{12}, immunoglobulin (IgG), and CA were used independently in this study. A vitamin B_{12} solution (0.015%) with 0.9% NaCl was first prepared. Approximately 1 ml of GCA microcapsules was immersed in 1 ml of vitamin B_{12} solution and kept in a water bath at 37°C and mixed at 120 rpm to facilitate ingress. At predetermined time intervals, 2 μl of the extra-capsular medium was withdrawn and the absorbance at 360 nm was measured using a NanoDrop 1000 UV–Vis spectrophotometer (Thermo Scientific, Wilmington, DE). By using a

Table 2. Various Microcapsule Samples with Respective Nomenclature

Chitosan-Alginate Coacervation Reaction Time (min)	Genipin Crosslinking Reaction Time (h)	200–300 μm	500–600 μm
15	6	SS-6	LS-6
	12	SS12	LS-12
	18	SS-18	LS18
30	6	SL-6	LL-6
	12	SL-12	LL-12
	18	SL-18	LL-18

calibration curve of vitamin B_{12} concentration vs. absorbance at 360 nm, the vitamin B_{12} concentration in the extra-capsular medium was estimated. The ingress mass transfer study was carried out until the system reached equilibrium. IgG was dissolved in 1× PBS to obtain a concentration of 0.40 mg/ml. Approximately 1 ml of GCA microcapsules was immersed in 3 ml of IgG solution and kept in a water bath at 37°C and mixed at 120 rpm to facilitate ingress. At predetermined time intervals, 2 μl of the extra-capsular medium was withdrawn and the protein concentration at 280 nm was measured using the Protein A280 module in a NanoDrop 1000 UV–Vis spectrophotometer. The ingress mass transfer study was carried out for ~3 days until the system reached equilibrium. Similarly, CA at a concentration of 0.65 mg/ml was prepared by dissolving in 1× PBS. Approximately 1 ml of the GCA microcapsules was immersed in 1 ml of CA solution and kept in a water bath at 37°C and mixed at 120 rpm to facilitate ingress. At predetermined time intervals, 2 μl of the extra-capsular medium was withdrawn and the protein concentration at 280 nm was measured using the Protein A280 module (extinction coefficient of 19.0%) in a NanoDrop 1000 UV–Vis spectrophotometer. The ingress mass transfer study was carried out until the system reached equilibrium.

Biomolecular egress from GCA microcapsules

First, CA at a concentration of 1.70 mg/ml was allowed to ingress into the GCA microcapsules as explained in the preceding section. After the system had reached equilibrium, the extra-capsular medium was removed completely and replaced with 1 ml of 1× PBS, thus allowing egress of CA from inside the GCA microcapsules into the extra-capsular medium. At predetermined time intervals, 2 μl of the extra-capsular medium was withdrawn and the protein concentration at 280 nm was measured using the Protein A280 module (extinction coefficient of 19.0%) in a NanoDrop 1000 UV–Vis spectrophotometer. The egress mass transfer study was carried out until the system reached equilibrium.

Scaling analysis to predict and compare membrane thickness

Recently, scaling analysis has been shown to effectively identify the dominant terms in an electrospray process.[26] Similarly, a scaling analysis was performed to understand the process that controls the membrane thickness based on the procedure described by Krantz.[27] The chitosan-alginate coacervation reaction was assumed to be first order, and the effects of curvature were ignored based on the assumption that the penetration is relatively small in comparison with the radius of the microcapsules. Hence, considering the one-dimensional, unsteady-state diffusion and reaction of chitosan within a stationary matrix of crosslinked alginate, the appropriate form of the species-conservation equation is given by the following:

$$\frac{\partial c_A}{\partial t} = D_{AS}\frac{\partial^2 c_A}{\partial y^2} - k_1 c_A \tag{4}$$

where c_A is the concentration of chitosan in moles per unit volume, y is the spatial coordinate measured from the interface of the microcapsule with the surrounding aqueous solution of chitosan, t is the temporal coordinate, k_1 is the reaction rate constant, and D_{AS} is the diffusion coefficient of chitosan in the crosslinked alginate matrix, which is assumed to be constant. The initial and boundary conditions are given by the following:

$$c_A = 0 \quad \text{at} \quad t \le 0 \tag{5}$$

$$c_A = \overset{\circ}{c_A} \quad \text{at} \quad y = 0 \quad 0 < t \le t_c \tag{6}$$

$$c_A = 0 \quad \text{at} \quad y = \delta_d \quad 0 < t \le t_c \tag{7}$$

where c_A^o is the equilibrium molar concentration of chitosan at the interface of the microcapsule and t_c is the contact time. Equation 7 states that the chitosan concentration drops to zero within some finite distance from the alginate matrix-solution interface δ_d. This thickness is determined by the ability of chitosan to diffuse into the crosslinked alginate matrix. Introduce the following dimensionless variables containing unspecified scale factors:

$$c_A^* \equiv \frac{c_A}{c_{As}}; \quad y^* \equiv \frac{y}{y_s}; \quad t^* \equiv \frac{t}{t_s} \tag{8}$$

Substitute these dimensionless variables into the describing equations and divide through by the dimensional coefficient of one term in each equation. As this is inherently an unsteady-state problem, divide through by the coefficient of the accumulation term:

$$\frac{\partial c_A^*}{\partial t^*} = \frac{D_{AS}t_s}{y_s^2}\frac{\partial^2 c_A^*}{\partial y^{*2}} + k_1 t_s c_A^* \tag{9}$$

$$c_A^* = 0 \quad \text{at} \quad t^* \le 0 \tag{10}$$

$$c_A^* = \frac{\overset{\circ}{c_A}}{c_{As}} \quad \text{at} \quad y^* = 0 \quad 0 < t^* \le \frac{t_c}{t_s} \tag{11}$$

$$c_A^* = 0 \quad \text{at} \quad y^* = \frac{\delta_d}{y_s} \quad 0 < t^* \le \frac{t_c}{t_s} \tag{12}$$

Set appropriate dimensionless groups equal to one to determine the scale factors:

$$\frac{\overset{\circ}{c_A}}{c_{As}} = 1 \quad \Rightarrow \quad c_{As} = \overset{\circ}{c_A} \tag{13}$$

$$\frac{\delta_d}{y_s} = 1 \quad \Rightarrow \quad y_s = \delta_d \tag{14}$$

Three time scales are determined by the two-dimensionless groups in Eq. 9 and the dimensionless group appearing in both Eqs. 11 and 12:

$$\frac{t_c}{t_s} = 1 \Rightarrow \quad t_s = t_c \text{ contact time} \tag{15a}$$

$$\frac{D_{AS}t_s}{\delta_d^2} = 1 \quad \Rightarrow \quad t_s \equiv t_d = \frac{\delta_d^2}{D_{AS}} \text{ diffusion time scale} \tag{15b}$$

$$k_1 t_s = 1 \quad \Rightarrow \quad t_s \equiv t_r = \frac{1}{k_1} \text{ reaction time scale} \tag{15c}$$

The appropriate time scale is the contact time t_c, that is, the time allowed for the chitosan to contact the alginate

matrix; hence, $t_s = t_c$. Because reaction cannot occur without chitosan diffusion, the unsteady-state term must balance the diffusion term, which then gives the penetration depth for the diffusion of chitosan:

$$\frac{\delta_d^2}{D_{AS} t_c} \cong 1 \quad \Rightarrow \quad \delta_d = K\sqrt{D_{AS} t_c} \tag{16}$$

where the proportionality constant K, which has a magnitude of order one, has been introduced to account for the approximate nature of scaling analysis. The dimensionless describing equations now become the following:

$$\frac{\partial c_A^*}{\partial t^*} = \frac{\partial^2 c_A^*}{\partial y^{*2}} + k_1 t_c c_A^* \tag{17}$$

$$c_A^* = 0 \quad \text{at} \quad t^* = 0 \tag{18}$$

$$c_A^* = 1 \quad \text{at} \quad y^* = 0 \tag{19}$$

$$c_A^* = 0 \quad \text{at} \quad y^* = 1 \tag{20}$$

The region wherein reaction occurs is thinner than the region wherein diffusion of chitosan has penetrated. Moreover, the reaction can begin only when diffusion causes chitosan to penetrate into the alginate. The reaction will go to completion only within the region wherein the contact time is greater than the sum of the diffusion time plus the reaction time. This provides a criterion for determining the thickness of the region wherein the chitosan reaction with the crosslinked alginate matrix has gone to completion. Hence, we have the following:

$$t_c = \frac{\delta_r^2}{D_{AS}} + \frac{1}{k_1} \quad \Rightarrow \quad \delta_r = K\sqrt{D_{AS}\left(t_c - \frac{1}{k_1}\right)} \tag{21}$$

Equation 21 allows determining the reaction rate constant k_1 by comparing the thickness of the shell wherein the reaction of chitosan with the crosslinked alginate matrix has gone to completion for two different contact times; that is,

$$\left[\frac{(\delta_r)_1}{(\delta_r)_2}\right]^2 = \frac{(t_c)_1 - \frac{1}{k_1}}{(t_c)_2 - \frac{1}{k_1}} \tag{22}$$

Once k_1 has been determined, Eq. 21 permits determining $K\sqrt{D_{AS}}$ that provides an estimate of the diffusion coefficient D_{AS} because $K \cong 1$.

Computational method to determine the characteristic time for diffusion

Initial (C_S^0), equilibrium (C_S^{eq}), and time-dependent ($C_S(t)$) concentrations of various biomolecules were measured according to the procedures described in the previous sections. The experimental data were fit to Eq. 1 for biomolecular egress and Eq. 2 for biomolecular ingress using the method of multidimensional unconstrained nonlinear minimization in MATLAB software to obtain the value of the characteristic time τ.

Results and Discussion

Fabrication and physical characterization of GCA microcapsules

The biomolecular mass transport across the GCA microcapsules is primarily affected by the microcapsule size, membrane thickness, and membrane crosslinking density. Each of these parameters was controlled in three serial steps as described below to investigate their effects on the biomolecular mass transport. First, the microcapsule size was controlled by the electrospray process as illustrated in Figure 1A. The electrospray technique is a proven, simple, and efficient method to produce spherical monodisperse droplets. For a range of nozzle voltages V_N, there exists a linear relationship between voltage and droplet size.[28] Hence, we varied V_N to obtain different sized droplets. Micro-dripping at a high V_N (11.5 kV) and medium flow rate was used to obtain small droplets (273.89 $\pm$ 23.79 μm in diameter) as it is known to provide a narrow size distribution by reducing the formation of satellite particles. To produce large size droplets (571.68 $\pm$ 30.24 μm in diameter), an additional ring voltage V_R was used to stabilize the electrospray, increase the droplet size, and provide monodispersity. The electrospray operating conditions required to obtain the small and large microcapsules are summarized in Table 1. Second, the membrane thickness was controlled by varying the chitosan–alginate coacervation reaction time (15 or 30 min). The calcium crosslinked alginate microcapsules when treated with chitosan resulted in a coacervation complex due to strong electrostatic interactions between the carboxyl groups in the alginate and the primary amine groups in chitosan as shown by Chen et al.[22] and pictorially represented in Figure 1B. This AC complex has been reported to be stronger than the conventional alginate–PLL binding. As genipin does not react with alginate, the genipin-chitosan membrane thickness was fixed depending on the chitosan-alginate coacervation reaction time. Third, the genipin-chitosan membrane density was controlled by varying the genipin crosslinking reaction time with chitosan (6, 12, or 18 h). The membrane formation is insensitive to changes in genipin concentration but highly sensitive to temperature.[22] As the GCA microcapsules were to be used for encapsulation involving live cells, we chose 37°C to maintain a favorable condition for crosslinking and to sustain cell viability during the process. The membrane formation step involving reaction of genipin with the chitosan shell was carried out resulting in the formation of a genipin crosslinked chitosan membrane shell with a noticeable color change from colorless to bluish purple (data not shown), the intensity of which depended on the reaction time. Genipin is known to react with chitosan's amino groups resulting in highly conjugated heterocyclic genipin derivatives that are bluish in color. In addition, reaction of the ester group in genipin with the amino group in chitosan could result in the formation of secondary amide linkages or crosslinking.[29]

Genipin-chitosan membrane characterization of GCA microcapsules

To further confirm the formation of a genipin crosslinked chitosan membrane shell as described earlier, the GCA microcapsules were viewed under a confocal microscope.

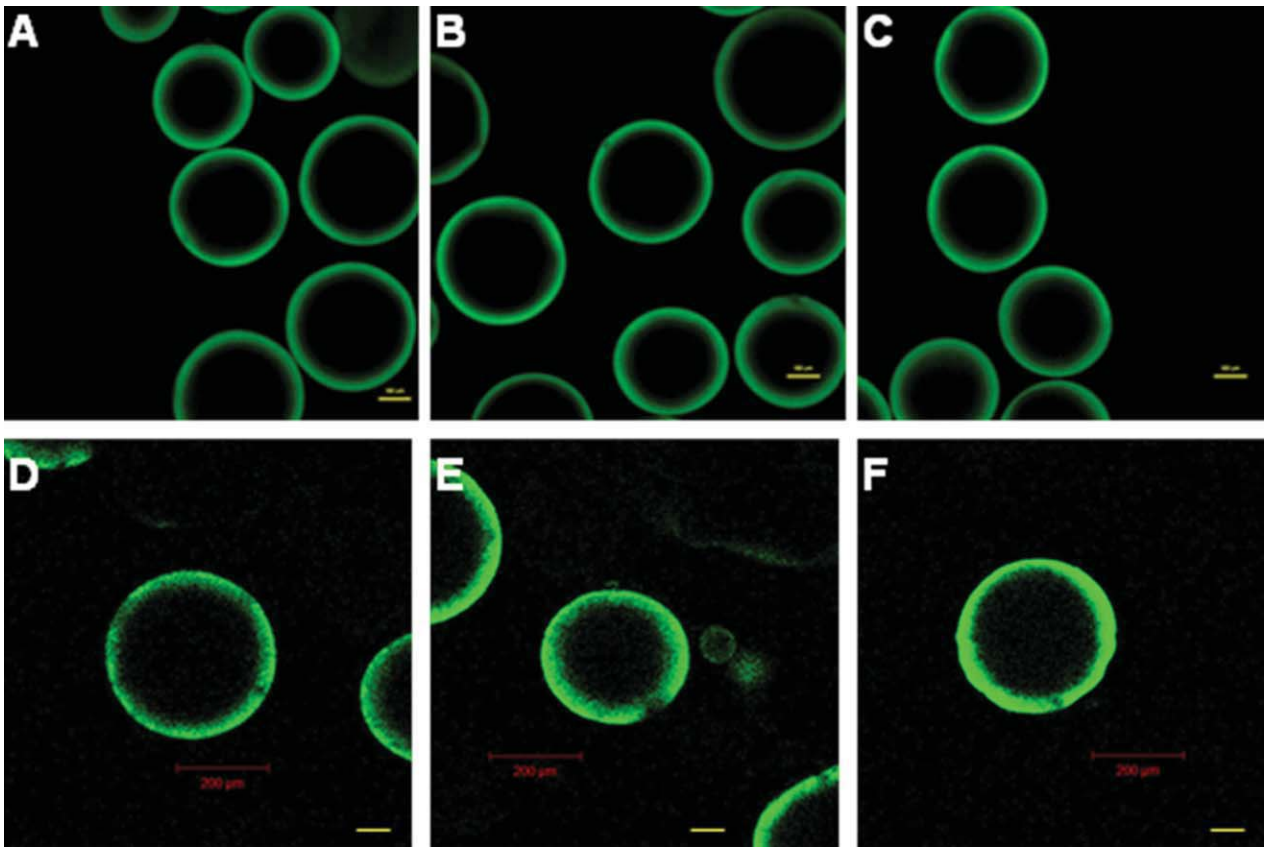

Figure 2. Representative confocal images of GCA microcapsules showing alginate core and genipin-chitosan membrane shell.

A: SS-6 microcapsules, (B) SS-12 microcapsules, (C) SS-18 microcapsules, (D) SL-6 microcapsules, (E) SL-12 microcapsules, and (F) SL-18 microcapsules. Bar represents 100 μm. [Color figure can be viewed in the online issue, which is available at wileyonlinelibrary.com.]

All the microcapsule samples in Figure 2 revealed an alginate core represented by the dark interior and the fluorescent genipin crosslinked chitosan membrane shell (green color). It is interesting to note that the microcapsules reacted with chitosan for 15 min possessed a similar membrane thickness irrespective of the changes in either genipin crosslinking reaction time or microcapsule size. Table 3 reveals the same for microcapsules reacting with chitosan for 30 min. From this, it is clear that within the domain of the chosen genipin crosslinking reaction times and microcapsule sizes, the membrane thickness is controlled only by the AC coacervation reaction time. Specifically, the genipin crosslinking time of 6 h is sufficient for genipin to fully penetrate the AC complex shell (for both 15 and 30 min of AC coacervation reaction time) in both small and large size microcapsules. Any further increase in the genipin crosslinking reaction time would only increase the crosslinking density of the membrane and not the thickness. This could be because genipin only interacts with chitosan already bound to the alginate. Thus, the membrane thickness is mainly controlled by the thickness of the AC complex that is limited by AC coacervation reaction time.

Recently, genipin's fluoregenic property has been exploited to characterize microcapsules. Because of the high specificity of the genipin, the fluorescent signals are due to genipin-chitosan conjugates rather than the AC complex or alginate core.[29] Similar results were observed in our study as seen in Figure 2 that shows a dramatic difference in the signal intensity between the alginate core and the membrane, the crosslinking density in the membrane was quantified by measuring the fluorescence intensity along randomly drawn lines across the microcapsule as shown in Figures 3A, B. The profiles also reveal very high signal intensity at the outer surface of the membrane, gradually decreasing toward the alginate core. The profiles also confirm the results from the confocal images in Figure 2 regarding the membrane thickness and its change with AC coacervation reaction time. From Figures 3A, B, it can be seen that with the increase in

Table 3. Average Genipin-Chitosan Membrane Thickness of Microcapsules

Microcapsule Samples	SS-6	SS-12	SS-18	SL-6	SL-12	SL-18
Membrane thickness (μm)	32.87 $\pm$ 4.40	33.11 $\pm$ 3.30	33.09 $\pm$ 3.41	60.56 $\pm$ 4.05	60.12 $\pm$ 3.56	58.46 $\pm$ 2.11
Microcapsule samples	LS-6	LS-12	LS-18	LL-6	LL-12	LL-18
Membrane thickness (μm)	33.87 $\pm$ 3.29	31.11 $\pm$ 3.10	32.91 $\pm$ 2.78	57.65 $\pm$ 4.41	58.28 $\pm$ 6.73	62.05 $\pm$ 4.39

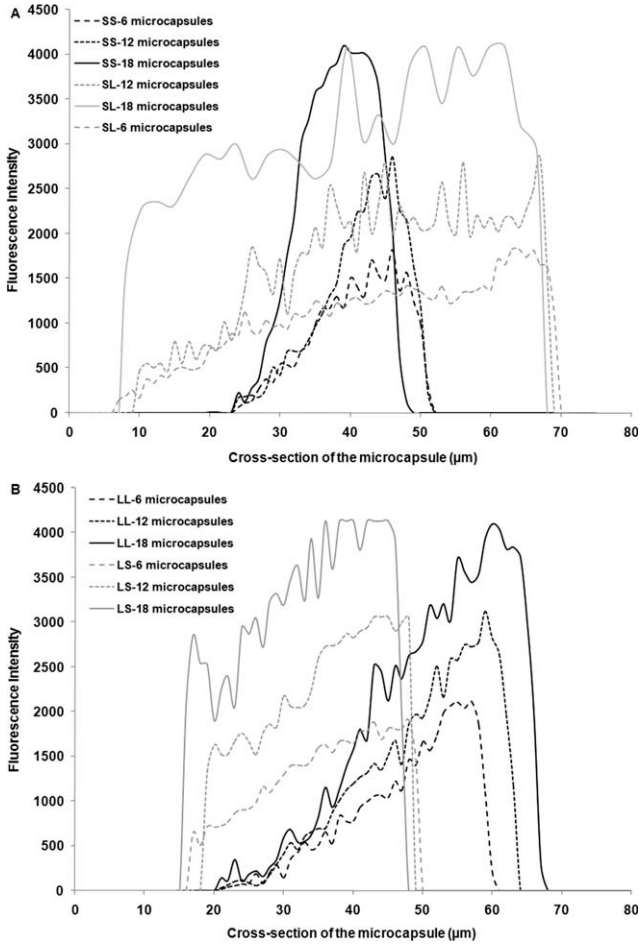

Figure 3. Fluorescence intensity profiles of GCA microcapsules along the cross section of the microcapsule.

A: Small microcapsules and (B) large microcapsules.

genipin crosslinking reaction time, the nonhomogeneity in the membrane density increases as indicated by the increasing slope in the profiles. This could be caused by the diffusion of genipin from the shell into the core of the microcapsule. The restricted diffusion of chitosan during the formation of the AC complex shell could also have resulted in a nonhomogeneous membrane and is consistent with other reports.[29] However, with longer crosslinking time, genipin penetrates deeper and forms more crosslinks, thus resulting in a more homogeneous and dense membrane as seen in Figure 3A.[21]

Prediction of membrane shell thickness

It is critical to control the thickness of the genipin-chitosan membrane shell due to the fact that it not only imparts capsular integrity but also controls biomolecular transport. Using Eq. 22, we first calculated the AC coacervation reaction constant (k_1) by using the known experimental results for the membrane thickness at two different AC coacervation reaction times as follows: $t_{c1} = 15$ min and the corresponding membrane thickness $\delta_1 = 33$ μm; $t_{c2} = 30$ min and the corresponding membrane thickness $\delta_2 = 60$ μm. Thus, the AC coacervation reaction constant (k_1) was calculated to be 0.118 min^{-1}. Subsequently, Eq. 21 was used to obtain $K\sqrt{D_{AS}} = 1.67 \times 10^{-6}$ cm^2/min. Because $K \cong 1$, the diffusion coefficient of chitosan in the alginate matrix is estimated to be $D_{AS} \cong 1.67 \times 10^{-6}$ cm^2/min. Now, using Eq. 21 with the known k_1 and $K\sqrt{D_{AS}}$ values, the membrane thickness at any given AC coacervation reaction time can be predicted. Moreover, Eq. 21 shows that the membrane thickness depends only on the reaction time and is independent of the microcapsule size. However, this predictive model can be used with confidence only within the range of microcapsule sizes and genipin crosslinking times used in this study. The model assumes that the distance of chitosan penetration in the alginate matrix is small in comparison to the radius of the microcapsule, which is confirmed by the measured membrane thicknesses.

Biomolecular ingress into GCA microcapsules

Figure 4 shows representative profiles of the experimental results of the ingress of vitamin B_{12} into the large LS microcapsules that had diameters in the range of 500–600 μm and a chitosan–alginate coacervation reaction time of 15 min. The error bars in Figure 4 were determined from the standard deviation of replicate experiments and are representative of the error in all the experiments reported here. The data for the three-dimensionless biomolecule concentrations shown in Figure 4 along with data for nine other microcapsules were fit to Eq. 2 to obtain the characteristic ingress time (τ) values summarized in Table 4. The experimental data fit the model very well with correlation coefficient (R^2) values close to 1. Ingress of vitamin B_{12} reaches equilibrium rapidly but at a different rate based on the type of microcapsule. Table 4 for vitamin B_{12} reveals that τ increases as the genipin crosslinking time of the microcapsules increases. Also, the diffusion is faster in microcapsules with a thinner membrane irrespective of the microcapsule size. It is also interesting to notice that at a given genipin crosslinking time

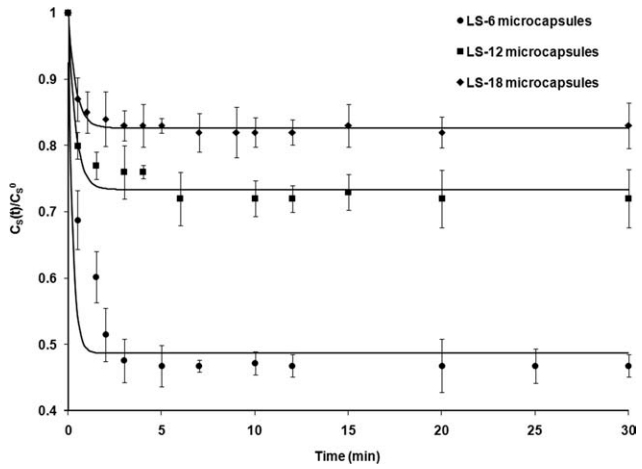

Figure 4. Representative plots of ingress of vitamin B_{12} into large GCA microcapsules.

The points are experimental data and the solid curves are the theoretical predictions from Eq. 2 for LS-6, LS-12, and LS-18, microcapsules with correlation coefficient (R^2) being 0.97, 0.94, and 0.98, respectively.

Table 4. The Calculated Characteristic Time (τ) from Eq. 2 for Biomolecular Ingress into GCA Microcapsules

Microcapsule Samples	Characteristic Time τ (min)		
	Vitamin B_{12}	Immunoglobulin	Carbonic Anhydrase
SS-6	0.09	–	1.73
SS-12	0.11	–	2.19
SS-18	0.13	–	2.41
SL-6	0.26	–	2.17
SL-12	0.42	–	2.35
SL-18	0.76	–	2.78
LS-6	0.23	668	1.49
LS-12	0.39	–	1.72
LS-18	0.41	–	2.26
LL-6	0.25	970	1.65
LL-12	0.49	–	1.92
LL-18	0.53	–	2.34

"–"represents negligible diffusion (complete exclusion) of IgG into the microcapsules and thus no curve fitting was performed.

and membrane thickness, the increase in microcapsule size seems to slow down the biomolecular transport (indicated by the increase in τ).

Figure 5 shows the IgG diffusion into the large LS-6 and LL-6 microcapsules that had diameters in the range of 500–600 μm and chitosan-alginate coacervation reaction times of 15 and 30 min, respectively. In contrast to the data for the large microcapsules shown in Figure 5, all of the small and most large microcapsules (LS-12, LS-18, LL-6, and LL-18) completely excluded IgG from ingress. However, the large microcapsules (LS-6 and LL-6) allowed very slow IgG ingress and revealed that with an increase in the membrane thickness, IgG diffuses more slowly as shown in Figure 5 and Table 5. The magnitude of τ for IgG ingress is at least three orders of magnitude larger than that for vitamin B_{12}.

Representative profiles of the ingress of CA through the large LS microcapsules that had diameters in the range of 500–600 μm and a chitosan–alginate coacervation reaction time of 15 min at different genipin crosslinking times are

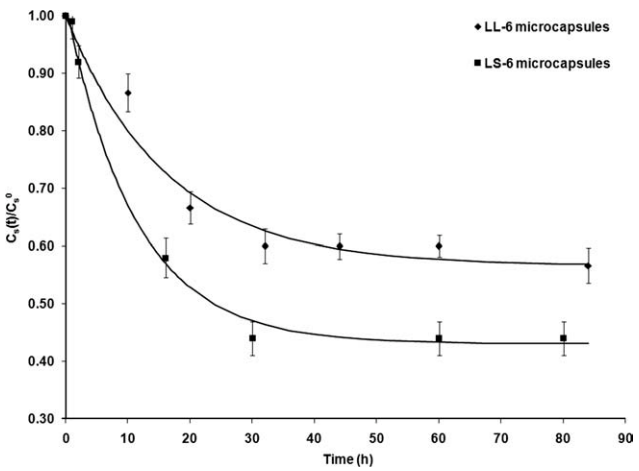

Figure 5. Representative plots of ingress of IgG into LS-6 and LL-6 microcapsules.

The points are experimental data and the solid curves are the theoretical predictions from Eq. 2 with correlation coefficient (R^2) being 0.99 and 0.97, respectively.

Table 5. Calculated Characteristic Time (τ) from Eq. 1 for Biomolecular (Carbonic Anhydrase) Egress

Microcapsule samples	Characteristic time τ (min)
SS-6	1.57
SS-12	2.99
SS-18	3.22
SL-6	1.77
SL-12	3.06
SL-18	3.29
LS-6	1.49
LS-12	1.87
LS-18	2.46
LL-6	1.49
LL-12	2.12
LL-18	2.54

shown in Figure 6. These profiles reveal that CA diffuses faster than IgG and reaches equilibrium in ~10–15 min. As expected, CA shows slower diffusion in microcapsules with higher genipin crosslinking time as shown by the τ values in Table 4. Also, the increase in membrane thickness slows down the CA ingress noticeably irrespective of microcapsule size. However, an important observation is that with an increase in the microcapsule size, diffusion of CA exhibits a completely opposite trend in comparison with vitamin B_{12}. Specifically, at any genipin crosslinking time and membrane thickness, τ decreases as the microcapsule size increases in case of CA ingress. This simply means that the ingress of CA is faster through the large microcapsules in comparison with the small microcapsules. The magnitude of τ for CA is at least one order of magnitude larger than that of vitamin B_{12}.

In microcapsule-based protein delivery for biomedical applications, it is important to ensure efficient inward diffusion of nutrients (oxygen, vitamins, etc.), exclusion of immune-macromolecules (antibodies), removal of waste products (ammonia, etc.) and most importantly, outward diffusion of the therapeutic protein into the target site. Keeping this in mind, in this study, we chose vitamin B_{12}, IgG, and

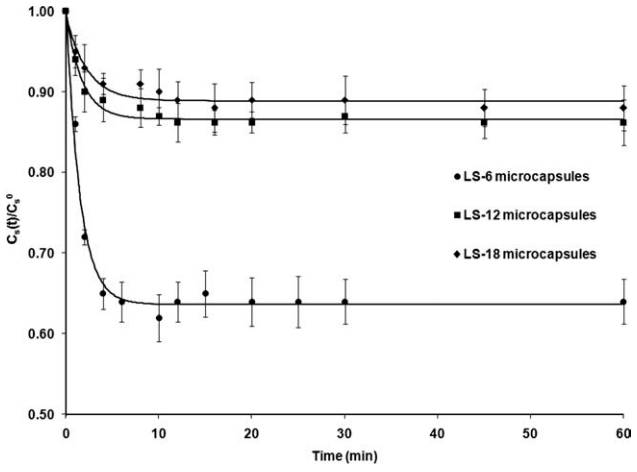

Figure 6. Representative plots of ingress of carbonic anhydrase into large GCA microcapsules.

The points are experimental data and the solid curves are the theoretical prediction from Eq. 2 for LS-6, LS-12, and LS-18, microcapsules with correlation coefficient (R^2) being 0.98, 0.98, and 0.95, respectively.

CA as model biomolecules representing a nutrient, an antibody, and a therapeutic protein, respectively. By varying the membrane properties (thickness and crosslinking density) and size of the microcapsules, the diffusive behavior of the biomolecules was evaluated. First, an increase in genipin crosslinking reaction time resulted in denser crosslinking and reduced the permeability, thus slowing down diffusion as indicated by an increasing τ for all the three biomolecules. As discussed earlier, the increase in genipin crosslinking time only increased the crosslinking density and not the membrane thickness (which was already fixed by the AC coacervation reaction time). However, because of the large size of IgG ($\sim$150 kDa), most of the microcapsules (except LS-6 and LL-6, which had the shortest genipin reaction times) completely excluded its ingress, thus confirming the desired permselectivity property. Note that the microcapsules that allowed IgG ingress had a less dense membrane (low crosslinking density). This underscores the importance of membrane crosslinking density in providing favorable permselectivity to the microcapsules. Moreover, the slowing down of the diffusion rate (increase in τ) of all the three biomolecules with an increase in membrane thickness can be attributed to the longer diffusion path length (or increased resistance to diffusion). Our study demonstrates a simple yet effective way to control the membrane thickness by varying the AC coacervation reaction time.

The mass transport behavior of the biomolecules with respect to the microcapsule size is intriguing. With an increase in microcapsule size, the tendency to swell resulted in increased permeability and diffusion path length. Vitamin B_{12} (M_W of 1.5 kDa) being a small molecule did not experience any effect of the increased permeability. Large microcapsules experienced relatively greater swelling in comparison with the small microcapsules; hence, the increase in diffusion path length resulted in an increase in τ. In contrast, in case of IgG and CA, the effect of increased permeability due to swelling resulted in faster diffusion despite a longer diffusion path length with an increase in microcapsule size. This indicates that diffusion of large molecules such as IgG (M_W of 150 kDa) and CA (M_W of 30 kDa) is controlled by the membrane permeability and not by the microcapsule size. Thus, small microcapsules that resist swelling and possess restricted permeability were able to slow down the diffusion of CA and in fact completely exclude the ingress of IgG. These results suggest that small GCA microcapsules are better suited both to improve inward diffusion of small nutrient molecules and completely exclude ingress of immune-macromolecules such as IgG. In addition, small GCA microcapsules have higher permselectivity in comparison to other microcapsules such as APA, Ba-alginate, and Ba-APA that can allow diffusion of molecules of molecular weight up to 300 kDa.[8]

Biomolecular egress from GCA microcapsules

Protein (CA) release from GCA microcapsules into the extra-capsular medium was measured, and the data were fit to Eq. 1 and the characteristic time τ obtained. Figure 7 shows representative data for the large LS microcapsules that had diameters in the range of 500–600 μm and a chitosan-alginate coacervation reaction time of 15 min. These

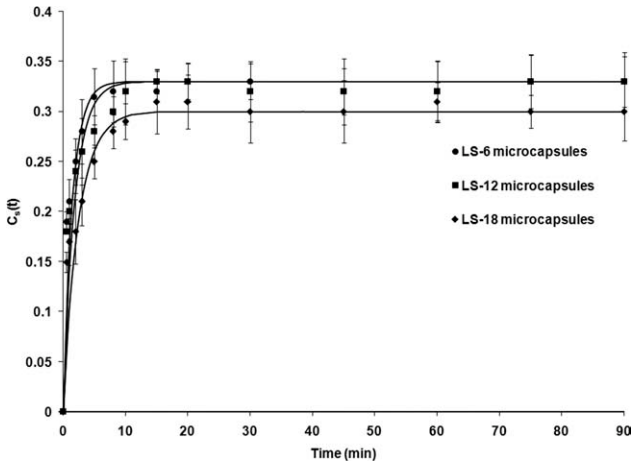

Figure 7. Representative plots of egress of IgG into large GCA microcapsules.

The points are experimental data and the solid curves are the theoretical predictions from Eq. 1 for LS-6, LS-12, and LS-18, microcapsules with correlation coefficient (R^2) being 0.97, 0.94, and 0.98, respectively.

data confirm the similarity in release rate between the egress and the ingress of CA. Table 5 summarizes the τ values for CA egress from all 12 GCA microcapsules that were studied. The egress of CA is observed to slow down (increase in τ) as the microcapsules are subjected to longer genipin crosslinking times. The membrane thickness has a similar effect. Irrespective of the membrane density and microcapsule size, an increase in membrane thickness decreases the diffusion rate of CA from the microcapsules. Similar to CA ingress, the size of the microcapsules has a noticeable effect on the egress. As the microcapsule size increases, the diffusion of CA from the microcapsules seems to get faster (decrease in τ). The increase in τ for large relative to small microcapsules was around 9–25%. Nonetheless, the magnitude of τ for CA egress is comparable with that of CA ingress.

Similar to CA ingress, CA egress from the microcapsules (small and large) is decelerated (increase in τ) with an increase in genipin crosslinking time due to the formation of denser crosslinks and reduced permeability. The decrease in τ as the microcapsule size increases is consistent with the CA ingress results, probably due to improved permeability resulting from swelling as explained previously. These results underscore the importance of small microcapsules that display less swelling and better mechanical stability despite slightly reduced egress of CA. Other microcapsules such as APA[9–11,30] and Ba-APA[8] have shown that neither the size nor the type of microcapsule affects the product egress significantly, which indicates low permselectivity. Two studies have shown that APA microcapsules with additional shell- or core-cross-linking[31] and AP-PMM_{50} microcapsules[32] possess a molecular weight cut-off (MWCO) of around 100–200 kDa by using Dextran molecular markers. The use of Dextrans to assess selectivity is not reflective of protein transport across the semi-permeable membrane due to factors such as surface charge, size variation for the same molecular weight, and conformation. Also, a high MWCO of 300 kDa for APA microcapsules[33] and 150–247 kDa for alginate-PLL-pectin-PLL-alginate microcapsules[34] has

been demonstrated, but this MWCO is not recommended for immunoisolation because the molecular weight of IgG is around 150 kDa. APA microcapsules treated with growth factors and collagen did not improve the selectivity as it partially allowed the ingress of proteins of 150–300 kDa,[10] whereas only erythropoietin (34 kDa) was shown to be secreted from APA microcapsules encapsulating myoblasts.[35] These studies demonstrate poor or no selectivity. APA microcapsules were shown to resist the diffusion of IgG, but the study was performed for only 1 h.[36] This experimental design and the analysis are erroneous because IgG is a macromolecule and its diffusion is slow. Typically, the diffusion should be monitored at least for 2–3 days to observe the real phenomena. However, one study by Yoshioka et al. has proven that APA(Ba) microcapsules completely excluded the ingress of components of anti-serum by demonstrating that the encapsulated cells were viable for at least 10 days.[36] This study shows that the antibodies in the anti-serum were excluded from ingress; however, it lacks a systematic approach to control the permeability and to confirm it as compared with our diffusion studies bolstered by the mathematical modeling. Also, the GCA microcapsules can be produced with considerable control over membrane thickness, density, and microcapsule size as demonstrated in this study. Because GCA microcapsules exhibit improved permselectivity, they could be better bioreactors for protein delivery in biomedical applications. However, this inference needs to be validated with the evaluation of GCA microcapsules in the presence of protein expressing cells. Also an optimization of GCA microcapsules in terms of protein secretion and long-term mechanical stability is warranted. Nevertheless, this study provides useful insight into the potential of GCA microcapsules with respect to nutrient diffusion, IgG exclusion, and protein release in addition to aspects of controlling membrane permeability.

Conclusions

In summary, GCA microcapsules were characterized and the effects of size, membrane density, and thickness on permselectivity to three relevant biomolecules were studied. The three-step electrospray process, chitosan-alginate reaction, and genipin crosslinking reaction were used to control the microcapsule size, membrane thickness, and density. Scaling analysis was implemented to obtain an equation that permitted obtaining the diffusion coefficient and rate constant from measurements of the chitosan–alginate reaction shell thickness as a function of contact time. The fluoregenic genipin-chitosan membrane enabled its vivid characterization in terms of thickness and density of crosslinking by the aid of confocal microscopic imaging. Furthermore, biomolecular mass transport across the GCA microcapsules was described by the use of mathematical models based on the balance of chemical potential of the biomolecule. Overall, the theoretical predictions fit the experimental results very well. GCA microcapsules allowed diffusion of small nutrient molecules (vitamin B_{12}) and protein (CA) but completely excluded large antibodies (IgG), thereby displaying improved selectivity compared to other microcapsule types. Microcapsules with denser and thicker membranes showed increased resistance to diffusion of all three biomolecules. Small microcapsules allowed better ingress of vitamin B_{12}, whereas large microcapsules favored the diffusion of IgG and CA due to swelling effects and the resultant increase in membrane permeability. Nevertheless, a follow-up study involving encapsulated cells in the alginate core should be carried out. This should encompass the detailed study on how membrane characteristics and microcapsule size affect protein expression and its subsequent release from the GCA microcapsules by using appropriate mathematical models.

Acknowledgments

The authors acknowledge the Biomedical Research Council (BMRC), A*STAR and the National University of Singapore for providing support under the grant numbers BMRC/07/1/21/19/508 and R279-000-257-731, respectively. The authors thank Malan Desai, Qiao Jian, Kan Fu, and Daphne Chen for technical assistance in the preparation of this manuscript.

Literature Cited

1. Lim F, Sun AM. Microencapsulated islets as bioartificial endocrine pancreas. *Science*. 1980;210:908–910.
2. Emerich DF, Winn SR, Hantraye PM, Peschanski M, Chen EY, Chu Y, McDermott P, Baetge EE, Kordower JH. Protective effect of encapsulated cells producing neurotrophic factor CNTF in a monkey model of Huntington's disease. *Nature*. 1997;386:395–399.
3. Prakash S, Chang TMS. Microencapsulated genetically engineered live *E. coli* DH5 cells administered orally to maintain normal plasma urea level in uremic rats. *Nat Med*. 1996;2:883–887.
4. Wollert KC, Drexler H. Cell-based therapy for heart failure. *Curr Opin Cardiol*. 2006;21:234–239.
5. Read TA, Sorensen DR, Mahesparan R, Enger P, Timpl R, Olsen BR, Hjelstuen MHB, Haraldseth O, Bjerkvig R. Local endostatin treatment of gliomas administered by microencapsulated producer cells. *Nat Biotechnol*. 2001;19:29–34.
6. Joki T, Machluf M, Atala A, Zhu J, Seyfried NT, Dunn IF, Abe T, Carroll RS, Black PM. Continuous release of endostatin from microencapsulated engineered cells for tumor therapy. *Nat Biotechnol*. 2001;19:35–39.
7. Lanza RP, Hayes JL, Chick WL. Encapsulated cell technology. *Nat Biotechnol*. 1996;14:1107–1111.
8. Peirone M, Ross CJD, Hortelano G, Brash JL, Chang PL. Encapsulation of various recombinant mammalian cell types in different alginate microcapsules. *J Biomed Mater Res*. 1998;42:587–596.
9. Rokstad AM, Holtan S, Strand B, Steinkjer B, Ryan L, Kulseng B, Skjak-Braek G, Espevik T. Microencapsulation of cells producing therapeutic proteins: optimizing cell growth and secretion. *Cell Transplant*. 2002;11:313–324.
10. Li AA, Shen F, Zhang T, Cirone P, Potter M, Chang PL. Enhancement of myoblast microencapsulation for gene therapy. *J Biomed Mater Res B*. 2006;77:296–306.
11. Zhang Y, Wang W, Xie Y, Yu W, Lu G, Guo X, Xiong Y, Ma X. Optimization of microencapsulated recombinant CHO cell growth, endostatin production, and stability of microcapsule in vivo. *J Biomed Mater Res B*. 2007;84:79–88.
12. Vandenbossche GM, Bracke ME, Cuvelier CA, Bortier HE, Mareel MM, Remon JP. Host reaction against empty alginate-polylysine microcapsules. Influence of preparation procedure. *J Pharm Pharmacol*. 1993;45:115–120.
13. Strand BL, Ryan TL, In't Veld P, Kulseng B, Rokstad AM, Skjak-Braek G, Espevik T. Poly-L-lysine induces fibrosis on alginate microcapsules via the induction of cytokines. *Cell Transplant*. 2001;10:263–275.
14. Fu SH, Hsu S, Chiou SC, Hsu BRS. Impact of cracks in alginate microcapsules on the survival of pancreatic islets. *Transplant Proc*. 2003;35:496.
15. Orive G, Hernandez RM, Gascon AR, Calafiore R, Chang TMS, de Vos P, Hortelano G, Hunkeler D, Lacik I, Pedraz JL. History, challenges and perspectives of cell microencapsulation. *Trends Biotechnol*. 2004;22:87–92.

16. Wheatley MA, Chang M, Park E, Langer R. Coated alginate microspheres: factors influencing the controlled delivery of macro-molecules. *J Appl Polym Sci*. 1991;43:2123–2135.
17. Bartkowiak A, Hunkeler D. New microcapsules based on oligoelectrolyte complexation. *Ann NY Acad Sci*. 1999;875:36–45.
18. Haque T, Chen H, Ouyang W, Martoni C, Lawuyi B, Urbanska A, Prakash S. Investigation of a new microcapsule membrane combining alginate, chitosan, polyethylene glycol and poly-L-lysine for cell transplantation applications. *Int J Artif Organs*. 2005;28:631–637.
19. Sung HW, Huang RN, Huang LLH, Tsai CC. In vitro evaluation of cytotoxicity of a naturally occurring crosslinking reagent for biological tissue fixation. *J Biomater Sci Polym Ed*. 1999;10:63–78.
20. Djerassi C, Gray JD, Kincl FA. Naturally occurring oxygen heterocyclics 9: isolation and characterization of genipin. *J Org Chem*. 1960;25:2174–2177.
21. Chen H, Ouyang W, Lawuyi B, Prakash S. Genipin cross-linked alginate-chitosan microcapsules: membrane characterization and optimization of cross-linking reaction. *Biomacromolecules*. 2006;7:2091–2098.
22. Chen H, Ouyang W, Jones M, Metz T, Martoni C, Haque T, Cohen R, Lawuyi B, Prakash S. Preparation and characterization of novel polymeric microcapsules for live cell encapsulation and therapy. *Cell Biochem Biophys*. 2007;47:159–167.
23. Takashi S, Takao Y, Seiji S, Kimio I, Toshiaki D. Permeability of azo-dye through poly(urea-urethane) microcapsule membrane. *J Membr Sci*. 2003;213:25–31.
24. Kaminski K, Zazakowny K, Szczubialka K, Nowakowska M. pH-sensitive genipin-cross-linked chitosan microspheres for heparin removal. *Biomacromolecules*. 2008;9:3127–3132.
25. Qi W, Ma J, Liu Y, Liu X, Xiong Y, Xie Y, Ma X. Insight into permeability of proteins through microcapsule membrane. *J Membr Sci*. 2006;269:126–132.
26. Xie J, Rezvanpour A, Wang CH, Hua J. Electric field controlled electrospray deposition for precise particle pattern and cell pattern formation. *AIChE J*. 2010;56:2607–2621.
27. Krantz WB. *Scaling Analysis in Modeling Transport and Reaction Processes—A Systematic Approach to Model Building and the Art of Approximation*. New York: Wiley, 2007.
28. Xie J, Wang CH. Electrospray in the dripping mode for cell microencapsulation. *J Colloid Interface Sci*. 2007;312:247–255.
29. Chen H, Ouyang W, Lawuyi B, Martoni C, Prakash S. Reaction of chitosan with genipin and its fluoregenic attributes for potential microcapsule membrane characterization. *J Biomed Mater Res A*. 2005;75A:917–927.
30. Ross CJC, Chang PL. Development of small alginate microcapsules for recombinant gene product delivery to the rodent brain. *J Biomater Sci Polym Ed*. 2002;13:953–962.
31. Mazumder MAJ, Burke NAD, Shen F, Potter MA, Stover HDH. Core-cross-linked alginate microcapsules for cell encapsulation. *Biomacromolecules*. 2009;10:1365–1373.
32. Gardner CM, Burke NAD, Stover HDH. Cross-linked microcapsules formed from self-deactivating reactive polyelectrolytes. *Langmuir*. 2010;26:4916–4924.
33. Awrey DE, Tse M, Hortelano G, Chang PL. Permeability of alginate microcapsules to secretory recombinant gene products. *Biotechnol Bioeng*. 1996;52:472–484.
34. Ouyang W, Chen H, Jones ML, Haque T, Martoni C, Afkhami F, Prakash S. Novel multi-layer APPPA microcapsules for oral delivery: preparation conditions, stability and permeability. *Indian J Biochem Biophys*. 2009;46:491–497.
35. Ding HF, Liu R, Li BG, Lou JR, Dai KR, Tang TT. Biologic effect and immunoisolating behavior of BMP-2 gene-transfected bone marrow-derived mesenchymal stem cells in APA microcapsules. *Biochem Biophys Res Commun*. 2007;362:923–927.
36. Yoshioka Y, Suzuki R, Oka H, Okada N, Okamoto T, Yoshioka T, Mukai Y, Shibata H, Tsutsumi Y, Nakagawa S, Miyazaki J, Mayumi T. A novel cytomedical vehicle capable of protecting cells against complement. *Biochem Biophys Res Commun*. 2003;305:353–358.

Manuscript received May 28, 2010, revision received Oct. 18, 2010, and final revision received Dec. 16, 2010.